Pressure Dependence of Amide Hydrogen−Deuterium Exchange Rates for Individual Sites in T4 Lysozyme†

T. Kevin Hitchens and Robert G. Bryant*

Department of Chemistry, University of Virginia, Charlottesville, Virginia 22901

Received December 2, 1997; Revised Manuscript Received February 25, 1998

ABSTRACT: We report measurements of the pressure dependence of rate constants for the exchange of amide residue protons with solvent deuterium for T4 lysozyme. Data obtained at nine pressures from 0.1 to 200 MPa are analyzed using an elementary kinetic model and the formalism of transition state theory which yield activation volumes for the exchange process. Resolution of individual amide sites was accomplished using the HSQC two-dimensional (2D) NMR experiment on uniformly ^{15}N-labeled protein. The observed activation volumes span the range from 2.75 to −25.1 mL/mol at 22 °C and pH* 7.5. When corrected for the pressure dependence of the ionic product for water and for the reported activation volume for the amide exchange reaction in model compounds, the portion of the activation volume associated with the accessibility of the solvent or catalyst to the amide sites ranges from −15.1 to 12.8 mL/mol. There is no simple correlation between the activation volumes and the protection factors for amide hydrogen exchange. The activation volumes for residues in close proximity in either the primary sequence or the folded structure may differ considerably. There is no trivial correlation between the activation volume and the secondary structural unit in which a residue is located, and activation volumes for residues that are apparently structurally coupled may be very different. The modest sizes of the activation volumes obtained under these conditions are in contrast to large values reported for bovine pancreatic trypsin inhibitor at more extreme conditions of 60 °C and pH* 8 where major unfolding events or structural rearrangements may dominate the mechanism [Wagner, G. (1983) *Q. Rev. Biophys. 16*, 1−57].

X-ray crystallographic and NMR studies have provided an extensive library of protein structure. However, the structures by themselves generally fail to provide a detailed picture of protein function or chemical catalysis because the functionally essential conformational reorganizations are not indicated by the static or dynamically averaged structures available.

Several experimental approaches demonstrate conformational flexibility within the protein structure. The exchange of the amide hydrogen atoms demonstrated early that even sites buried in the folded protein became available to the solvent or exchange catalyst if given enough time (*1*, *2*). Similarly, chemical modifications of apparently buried SH groups (*3*) seem to require structural flexibility. More rapid fluctuations were demonstrated by penetration of dioxygen molecules into protein interiors for quenching fluorescence (*4*) and by rapid 180° ring flips of buried aromatic side chains (*5*).

There are two fundamentally different types of measurement. Structures derived from X-ray crystallography provide superposition of structural snapshots. Other techniques such as solution phase NMR provide a time-averaged structure. In both cases, rarely populated structures make essentially no contribution to the structural result. On the other hand, the chemical reaction strategies such as buried SH group reactivity or amide hydrogen exchange may effectively integrate over the time course of protein structural fluctuations and record a rare structural fluctuation that permits a reaction or exchange event to occur. These chemical approaches are, therefore, sensitive to events that populate rarely sampled conformational states of the protein, which may be significantly different from the native or average structure of the molecule.

Amide hydrogen exchange measurements with solvent are particularly sensitive measures of structural fluctuations because the protein fold typically spreads the rate constants for the exchange over 8 orders of magnitude. Further, two-dimensional (2D) NMR methods now permit detection of many if not all of the individual amide positions in the protein; thus, there are approximately as many structural spies as there are amino acids in the protein. The hydrogen exchange experiment has been reviewed extensively elsewhere (*6*−*9*). There are two basic ideas about the mechanism of hydrogen exchange that differ in the extent and cooperativity of the structural rearrangement required for exchange of the amide hydrogen. One emphasizes penetration of solvent and/or catalyst and the other an apparently more cooperative local unfolding.

The temperature dependence of amide exchange rates provides powerful mechanistic insight. At room temperature, the hydrogen exchange at many amide sites is characterized by an activation energy on the order of 20 kcal/mol; at higher

† This work was supported by National Institutes of Health Grant GM 34541 and by the University of Virginia.

* Address correspondence to Robert G. Bryant, Department of Chemistry, University of Virginia, Charlottesville, VA 22901. Telephone: (804) 924-1494. Fax: (804) 924-3567. E-mail: rgb4g@virginia.edu.

S0006-2960(97)02950-4 CCC: $15.00
Published on Web 04/11/1998

temperatures, where the protein is less stable, the activation energy is much larger, which suggests that contributions from pathways involving greater degrees of cooperative unfolding are more important or accessible (*10*). Although not widely studied, the pressure dependence of amide hydrogen exchange rates in folded proteins may provide important information about protein fluctuations as well as about the mechanism for the exchange process.

Although very widely used, transition state theory and its several refinements may be questioned (*11*, *12*). The pressure dependence of a kinetic barrier may be derived from sources not apparent or even properly treated by the transition state formalism. However, in this study, the inherent chemical reaction of an amide proton exchanging with the solvent protons or deuterons is rapid, particularly at pH values above 7. Indeed, many sites exchange with solvent before we may measure them conveniently. In contrast, the exchange rates we report here for specific sites in the folded protein are slow, which leads to the hypothesis that solvent or base accessibility to the site dominates the observed rate. Either the protein must unfold locally, or the solvent or base must penetrate the compact protein structure before an exchange event may occur. It appears to be reasonable, in this case, to think of volume changes associated with the structural rearrangements required by either type of mechanistic pathway as potentially important. The activation parameters for transition state theory are easily extended to include the pressure−volume contribution to the activation free energy. As a consequence, the $P\Delta V^{\ddagger}$ represents the pressure−volume work required to achieve the configuration of the activated complex, which in this case reasonably involves the structural rearrangements required for access of the solvent or base to the buried amide proton sites. Nevertheless, in condensed phases, $P\Delta V^{\ddagger}$ values are generally small even at substantial pressures; experimentally, this fact requires precise temperature control for minimization of the usually dominant effects of temperature changes on the observed reaction rates.

In summary, we report here the first extensive study of the pressure dependence of individual and resolved amide hydrogen exchange rate constants. We report results expressed as activation volumes for 44 different sites in bacteriophage T4 lysozyme over the range from 0.1 to 200 MPa. We analyze these data from the perspective of transition state theory because it provides a useful parametrization of the data and a useful platform from which to discuss the results. T4 lysozyme provides an excellent protein for this series of studies because (1) large amounts of protein may be isolated from a bacterial expression system (*13*), (2) ^{15}N and ^{1}H NMR chemical shift assignments have been reported (*14*, *15*), and (3) this protein has been the subject of many structural and dynamical studies involving NMR and X-ray crystallography (*16*−*18*).

MATERIALS AND METHODS

T4 Lysozyme Preparation. The plasmid containing the gene encoding the C54T/C97A variant of T4 lysozyme was obtained from F. W. Dahlquist (University of Oregon, Eugene, OR; *14*, *16*, *19*). Both the stability and structure of this thiol-free variant (WT*) are similar to those of the wild-type T4 lysozyme. T4 lysozyme with uniform ^{15}N enrichment was produced with *Escherichia coli* bacteria grown on minimal medium with 1.0 g/L $^{15}NH_4Cl$ as the sole source of nitrogen (*13*). T4 lysozyme was prepared in 2 L batches with a Bioflow II Fermentor (New Brunswick Scientific, New Brunswick, NJ); 20−40 mg of protein was produced per liter of medium. Proir to exchange experiments, a stock solution of T4 lysozyme was prepared by combining protein from several protein preparations and dialyzing against 50 mM TRIS (pH 7.2) and 0.02% sodium azide.

High-Pressure Apparatus. A manually operated piston−screw−pump pressure generator (model 31-5.75-75) and a high-pressure reactor vessel (model R1-6-100) system was purchased from High-Pressure Equipment Co. (Erie, PA). Water was used as the compression fluid. A NesLab RTE 111 (±0.01 °C) temperature controller was used to circulate water through 50 ft of $^{1}/_{4}$ in. outside diameter copper tubing tightly wrapped around the pressure vessel that was in turn insulated with $^{1}/_{2}$ in. fiber glass insulation. The temperature of the pressure vessel was pre-equilibrated at 22 °C before each kinetic experiment. Pressure was determined with a AstraGauge pressure gauge (Astra Corp., Ivyland, PA) rated at 0.25% accuracy.

Sample tubes were constructed of blown glass starting from a 15 mm section of a 10 mm NMR tube. One end was sealed with the torch; a 6 mm length of 5 mm outside diameter glass tubing was attached to the other end to resemble a small round-bottom flask with a total volume of approximately 1 mL. The sample tube closures were fabricated from Imperial Eastman poly flow 44-p-1/4 tubing cut to a length of approximately 2 cm and thermally sealed at one end with a hot soldering iron. When the cap and tube are assembled, as long as there is no air trapped in the sample tube, there is no pressure differential across the sample tube because the pressure is applied to the protein solution by compression of the plastic closure.

Amide Hydrogen Exchange Experiments. Aliquots (1 mL) from a stock solution of 4.3 mg/mL protein in 50 mM TRIS buffer/H_2O (pH 7.2) and 0.02% sodium azide in H_2O were lyophilized. The lyophilized sample was rehydrated with 1 mL of D_2O (99.9% at. % D, CIL, Andover, MA) and the pH* (uncorrected meter reading) adjusted to 7.5, using a Sensorex mini pH electrode operating with an Orion pH meter (model 720A). The sample tube was filled with the rehydrated protein sample, and the closure tube was filled with TRIS/D_2O buffer (pH* 7.5). The cap and tube were assembled so that no air bubbles were trapped in the tube, and the assembled sample was sealed in a latex balloon. Five minutes was required to prepare the sample, place it in the pressure vessel, and bleed air from the pressure vessel. The desired pressure was achieved in a fixed time of 30−50 s depending on the pressure target. The amide exchange rates were measured for pressures from atmospheric pressure to 200 MPa, with increments of 25 MPa, at 22 °C using exchange times from 10 min to 3 h. Because the heat capacity of the pressure vessel and the associated thermostat is large and because the exchange times are long, any temporary increase in sample temperature caused by compression is minimal, and the effects on the measured rate constants negligible. After the exchange time, the protein samples were rapidly returned to atmospheric pressure and the pH* was adjusted to the exchange minimum (pH_{min} 3.2) with DCl to quench the exchange. Protein solutions were

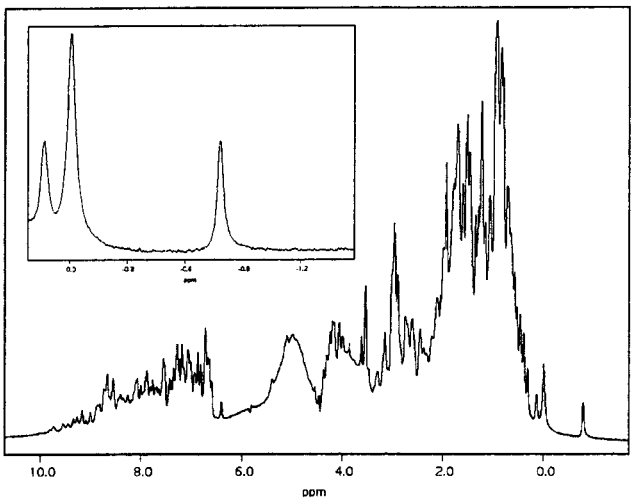

FIGURE 1: ^{1}H NMR spectrum of WT* T4 lysozyme in D_2O at pH* 3.2 and 25 °C obtained at 500 MHz. The expanded region (inset) shows the H^γ resonance of Val94 (−0.78 ppm) that is used to normalize concentrations for different samples.

concentrated by ultrafiltration using Centricon-10 microfiltration units (Amicon Corp., Danvers, MA) to a final volume of 250 μL for the NMR experiments. The resulting protein concentration was approximately 0.9 mM. Shigemi susceptibility-matched NMR tubes (Shigemi, Inc., Allison Park, PA) were used for all NMR measurements. For all high-pressure experiments, a constant 5 min sample preparation time between rehydration with D_2O and application of pressure was used, and 1 min was required to remove the sample from the pressure apparatus and titrate the sample pH to 3.2. Any exchange during the sample preparation and quenching time was accounted for by the $t = 0$ (6 min) reference sample, which was treated identically. The same protein stock solution was used for all kinetic runs from atmospheric pressure to 150 MPa of applied pressure. For the 175 and 200 MPa experiments, a second stock solution was prepared by recycling samples already studied by dialysis in H_2O buffer for several days. Amide proton HSQC peak intensities of the recycled protein were consistent with those of the reference spectrum, indicating complete back-exchange of the amide protons.

NMR Measurements. All ^{1}H NMR data were recorded at 500 MHz using a Varian Unity Plus 500 spectrometer. Data were processed using FELIX 95.0 NMR software (Biosym/Molecular Simulations, San Diego, CA). The amide hydrogen populations, which remained after a particular exchange time, were measured from the intensities of ^{15}N−^{1}H cross-peaks in an HSQC spectrum (*20*). The peaks were assigned on the basis of reported chemical shifts (*14*, *21*), and any ambiguity was clarified with the H^α chemical shifts with a HNHA experiment (*22*). HSQC peak intensities of different samples were normalized for differences in protein concentration and spectrometer hardware fluctuations using the peak intensity for the H^γ resonance of Val94 (−0.78 ppm) from a one-dimensional (1D) ^{1}H spectrum (*15*), acquired immediately following acquisition of the HSQC spectrum. As shown in Figure 1, this resonance peak is the highest-frequency resonance for T4 lysozyme, is well resolved, and served as an internal spin concentration reference that was used to normalize intensity measurements of all samples.

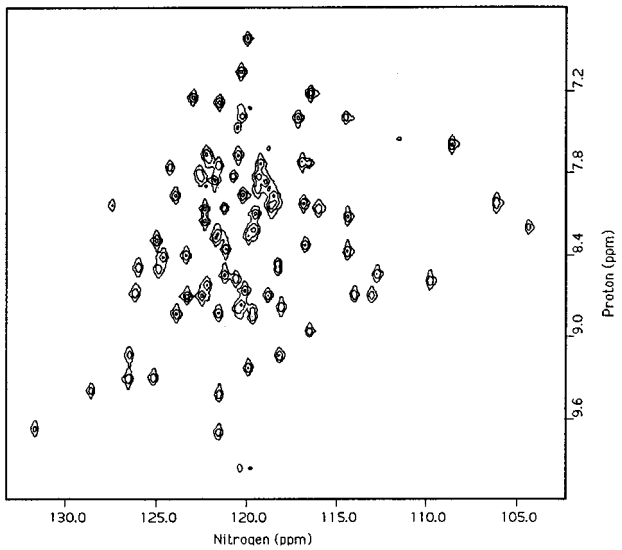

FIGURE 2: Reference HSQC spectrum obtained at 500 MHz of uniformly ^{15}N-enriched WT* T4 lysozyme in D_2O at pH* 3.2 and 25 °C obtained after a 6.0 min exchange period at pH* 7.5 with 0.1 MPa of pressure and 22 °C.

HSQC spectra were acquired with a ^{1}H spectral width of 5000 Hz. Each FID consisted of 1024 complex points collected with 32 transients. The ^{15}N spectral width was 1900 Hz, and a total of 512 complex points were collected in the t_1 time domain. HSQC data sets were acquired in approximately 5 h. The data were processed with a 90° shifted sine-squared apodization applied in both dimensions, and a linear baseline correction was applied in both dimensions.

The 1D ^{1}H spectra were acquired with 64 transients and a recycle delay of 7 s. Residual solvent and the TRIS methyl resonances were removed using a circular shift in the time domain and convolution-based solvent suppression. The data were transformed with 2 Hz exponential line broadening, and a second-order polynomial baseline correction was performed by picking baseline points flanking the Val94 H^γ resonance. The intensity of this 1D peak was obtained using the peak fitting software within FELIX 95.0.

Data Analysis. HSQC cross-peaks were normalized with the Val94 H^γ for the 1D ^{1}H NMR spectrum. The activation volumes were determined by fitting the normalized peak intensities obtained from 60 exchange experiments at nine different pressures to eq 1 using the nonlinear least-squares program NONLIN (*23*).

$$I(t) = I_o e^{-tk_o e^{(-P\Delta V^\ddagger/RT)}} \quad (1)$$

The independent variables were the exchange time (t) and pressure (P) of exchange. The fitted parameters were the initial intensity (I_o), the exchange rate constant at no applied pressure (k_o), and the observed activation volume $\Delta V^\ddagger_{obs}$. Individual rate constants were determined by fitting normalized peak intensities to a single-exponential function using the same software.

RESULTS AND DISCUSSION

The reference HSQC spectrum shown in Figure 2 was recorded after a 6 min exchange period at 1 atm and pH* 7.5, the time necessary for sample handling in a kinetic run

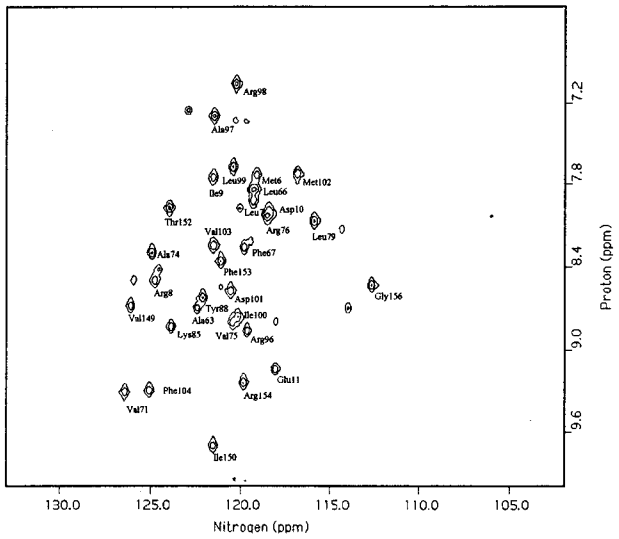

FIGURE 3: HSQC spectrum obtained at 500 MHz for uniformly ^{15}N-enriched WT* T4 lysozyme after a 90 min exchange period at pH* 7.5 and 22 °C in D_2O with 200 MPa of applied pressure. The spectrum was acquired at pH* 3.2, 25 °C, and atmospheric pressure. Assignments are indicated for residues of amide hydrogen sites that show little or no exchange over this period.

with a different applied pressure. Each peak of the HSQC spectrum corresponds to a ^{15}N−^{1}H directly bonded pair, and the peak intensity is directly proportional to the amide hydrogen population; hence, H → D exchange results in decreased ^{15}N−^{1}H peak intensity. Only the amide hydrogen sites that have slow to intermediate hydrogen exchange rates appear in Figure 2 because the rapidly exchanging amide sites fully exchanged with deuterium during the sample preparation time for the experiment. Nevertheless, 75 peaks are well resolved that permit unambiguous assignment.

The amide exchange rates in T4 lysozyme extend over 10 orders of magnitude. Figure 3 shows an HSQC spectrum acquired after a 90 min exchange period at 200 MPa. Even under these conditions, there are 29 amide proton resonances that exhibit little or no intensity decrease. These residues are well protected from hydrogen exchange at atmospheric pressure in the wild-type protein as well (*18*). Figure 4 depicts the position of these residues on a ribbon rendition of the native fold of the protein based on the X-ray crystal structure. These inert amide sites are centered about helix E (residues 93−105), which is well buried in a hydrophobic region of the helix bundle of the C-terminal domain. Helix E is the central helix in the hydrophobic core and is in close contact with helix A (residues 3−10), part of helix C (residues 60−79), helix D (residues 82−90), and part of helix H (residues 138−155). The slow exchange rate for these sites at atmospheric pressure is consistent with a lack of structural flexibility in this region of the protein. The observation that these sites remain inert at the highest pressure studied demonstrates that the protein structure remains essentially intact; i.e., there are no pressure-induced changes in this region of the protein that unfold the structure significantly.

Of the 160 residues with labile backbone amide hydrogen sites in T4 lysozyme, activation volumes for 75 amide sites could be determined in principle. Of these, the 31 sites mentioned above were not measured because of their slow rates, and 44 sites were well characterized. The remaining

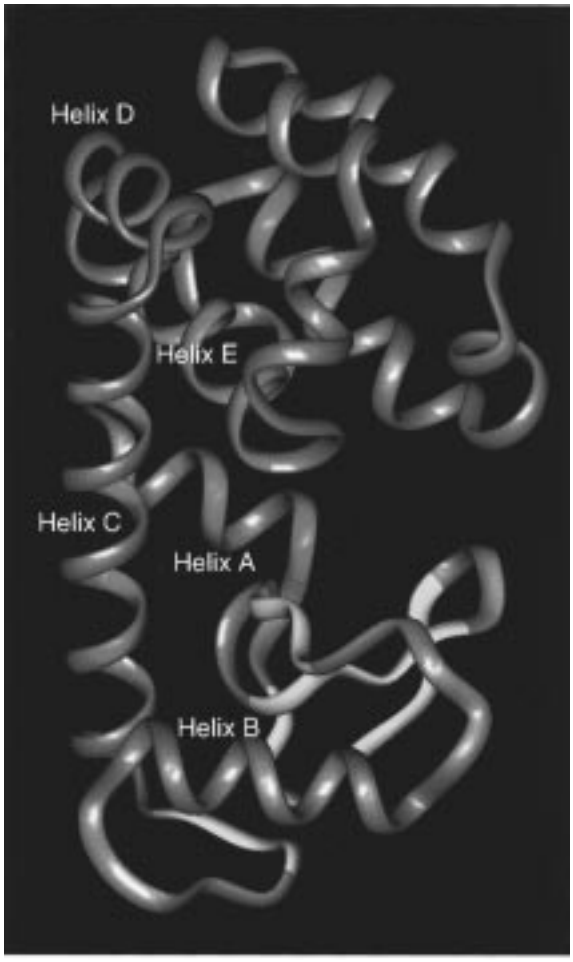

FIGURE 4: Ribbon diagram representation of the WT* T4 lysozyme structure derived from X-ray data. Red regions indicate the position of residues which show little or no hydrogen−deuterium exchange after 90 min at 200 MPa of applied hydrostatic pressure. The main helix structures are identified for reference, and the antiparallel β-sheet region is yellow.

85 sites were too labile to be measured accurately with the techniques of these experiments. The amide exchange rates were measured at nine pressures from atmospheric pressure to 200 MPa with six to eight exchange time periods per kinetic run ranging from 10 min to 3 h. The activation volume was extracted from the kinetic experiments by fitting all 60 data points simultaneously to eq 1. For the purpose of displaying the data, each kinetic run was also fit to a single-exponential equation, and Figure 5 shows a representative result. The activation volumes derived from this procedure are summarized in Table 1. Also shown are the protection factors, *P*, for the wild-type protein averaged over several pH conditions as reported by Dalquist (*18*). We note that the sites we have been able to characterize typically have protection factors between 3 and 7.

Examination of all the data shows that graphs of ln(k) versus pressure are linear within the error bars of each measurement. Although for some amide sites there may be a hint of nonlinearity, which could indicate a transition from one exchange mechanism to another with a different activation volume, the deviations are not sufficient to justify anything other than a linear approximation to the data given the errors. Wagner (*24*, *25*) measured the effect of pressure on exchange rates for the most slowly exchanging amide

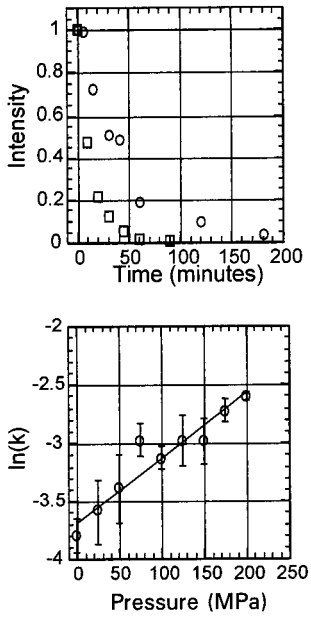

FIGURE 5: Kinetic data for the pressure dependence of the amide proton exchange rate constant for Leu46 in T4 lysozyme for exchange at pH* 7.5 and 22 °C. (Top) Plot of normalized intensity vs time for two kinetic runs: 0.1 MPa (1 atm) (○) and 200 MPa of applied pressure (□). (Bottom) Data from all pressures fit to eq 1. The slope of the line corresponds to a measured activation volume of -14.0 cm^3 mol^{-1}. Error bars represent a 67% confidence interval.

hydrogens in BPTI at 60 °C and pH 8 up to 300 MPa of applied pressure and observed a complicated dependence. Under these more extreme conditions, however, the hydrogen exchange rates of these residues are known to occur via the high-activation energy process at atmospheric pressure (*26*). The large values of activation volumes reported by Wagner (*25*) are consistent with more major structural rearrangements or unfolding expected for the high-energy pathway. However, because this mechanism is not dominant at 22 °C, the results cannot be compared to the present experiment.

Except for histidine 31, the amide hydrogen exchange rates increase with increasing pressure for all sites studied as indicated by the negative values for $\Delta V^{\ddagger}_{obs}$. His31 exhibits a small positive activation volume of 2.75 cm^3 mol^{-1}. Figure 6 is a plot of the measured activation volume versus the amino acid position in the primary amino acid sequence; secondary structural elements are also indicated. It is clear that the activation volumes may be significantly different for different residues even when they are nearest neighbors in the sequence. These results, which are derived from the advantages of new techniques and much greater resolution, are considerably different from the single aggregate value deduced by Carter et al. (*27*) 20 years ago. The observation that different residues have different activation volumes even when in close proximity suggests that the integrated effects of the structural fluctuations that result in amide hydrogen exchange are different for each residue. Nevertheless, we note that for the residues measured, the N-terminal domain, which includes the antiparallel β-sheet region of the protein, has a larger span of activation volumes than the C-terminal helix bundle region.

A second feature of these data is that there is an apparent minimum in the observed activation volumes between helix B (residues 39−50) and helix C (residues 60−79). However, a clear correlation between $\Delta V^{\ddagger}_{obs}$ and secondary structure type is not apparent. Furthermore, Table 1 reveals that there is no practical correlation between the observed activation volume and the protection factor.

Table 1: Measured Activation Volumes for WT* T4 Lysozyme for Applied Hydrostatic Pressures from 0.1 to 200 MPa[a]

residue	P	$\Delta V^{\ddagger}_{obs}$	confidence limits	$\Delta V_s + \Delta V^{\ddagger}_{k_{ex}}$	ΔV_s
Phe4	4.3	−10.3	−11.5, −9.1	10.6	−0.3
Lys16	6.0	−13.0	−14.6, −11.2	7.9	−3.0
Ile17	5.4	−13.7	−14.8, −12.5	7.2	−3.7
Tyr18	4.7	−6.4	−7.9, −4.9	14.5	3.6
Thr26	6.8	−12.7	−14.3, −11.1	8.2	−2.7
Ile27	6.8	−22.9	−25.4, −20.4	−2.0	−12.9
Gly28	6.3	−10.7	−12.1, −9.3	10.2	−0.7
Ile29	5.0	−14.4	−15.9, −12.8	6.5	−4.4
His31	6.1	2.75	0.9, 4.7	23.7	12.8
Leu33	6.0	−3.41	−5.1, −1.7	17.5	6.6
Lys43	4.8	−3.37	−6.0, −0.4	17.5	6.6
Glu45	5.2	−12.3	−14.0, −10.6	8.6	−2.3
Leu46	6.0	−14.0	−16.0, −12.0	6.9	−4.0
Asp47	6.4	−19.3	−20.5, −18.1	1.6	−9.3
Lys48	5.4	−15.6	−17.0, −14.2	5.3	−5.6
Ala49	5.4	−19.8	−21.3, −18.1	1.1	−9.8
Ile50	6.3	−21.2	−22.5, −20.0	−0.4	−11.3
Ile58	6.9	−25.0	−26.8, −23.2	−4.1	−15
Thr59	6.8	−20.0	−21.7, −18.9	0.9	−10.0
Glu62	4.3	−18.3	−19.7, −16.9	2.6	−8.3
Glu64	5.1	−9.6	−11.4, −7.7	11.3	0.4
Lys65	4.2	−14.9	−17.0, −12.7	6.0	−4.9
Asp70	6.3	−17.8	−20.0, −15.7	3.1	−7.8
Asp72	5.6	−9.13	−11.8, −6.4	11.8	0.9
Ala73	5.2	−9.20	−10.8, −7.5	11.7	0.8
Gly77	6.2	−8.64	−10.1, −7.1	12.3	1.4
Ile78	6.3	−7.64	−9.7, −5.5	12.4	1.5
Arg80	5.0	−9.22	−10.4, −8.0	11.7	0.8
Asn81	5.3	−14.1	−15.5, −12.6	6.8	−4.1
Leu84	5.3	−16.3	−18.1, −14.5	4.6	−6.3
Asp89	5.0	−10.3	−11.9, −8.7	10.6	−0.3
Leu91	6.2	−14.6	−16.9, −12.3	6.3	−4.6
Met106	5.5	−10.5	−12.8, −8.1	10.4	−0.5
Gln123	4.7	−25.1	−36.8, −18.8	−4.2	−15.1
Trp126	4.5	−12.7	−13.9, −11.5	8.2	−2.7
Ala129	5.5	−14.6	−16.3, −12.9	6.3	−4.6
Val131	5.0	−11.2	−18.1, −4.3	9.7	−1.2
Ala146	5.1	−13.2	−14.5, −11.8	7.7	−3.2
Lys147	4.5	−7.4	−8.5, −6.3	13.5	2.6
Val149	4.3	−16.6	−21.3, −11.9	4.3	−6.6
Thr151	5.2	−6.48	−7.5, −5.4	14.4	3.5
Thr155	5.0	−8.83	−10.5, −7.1	12.1	1.2
Thr157	5.7	−19.2	−20.8, −17.6	1.7	−9.2
Tyr161	5.6	−18.7	−20.9, −16.5	2.2	−8.7

[a] Activation volumes (cm^3 mol^{-1}) are reported with a 67% confidence limit. The protection factors are the average of measurements at several pH values and 1 atm of pressure for the wild-type protein (*18*).

An Analytical Model. The local unfolding model has proven useful in describing hydrogen exchange kinetics (*1*, *9*, *28*). If we assume that each individual amide site establishes an equilibrium between a closed and an open state, we may write

$$\text{closed} \underset{k_{-1}}{\overset{k_1}{\rightleftharpoons}} \text{open} \xrightarrow{k_{ex}} \text{exchange} \qquad (2)$$

where the amide hydrogen is protected from exchange in the closed form and may only exchange from the open state. Under the conditions of this experiment (pH > pH$_{min}$), the chemical exchange step may be approximated by $k_{ex} = k_{OH}[OH^-]$. A penetration model may be formulated similarly, where access of the solvent and or catalyst is dependent on movement of one or more residues that may define the

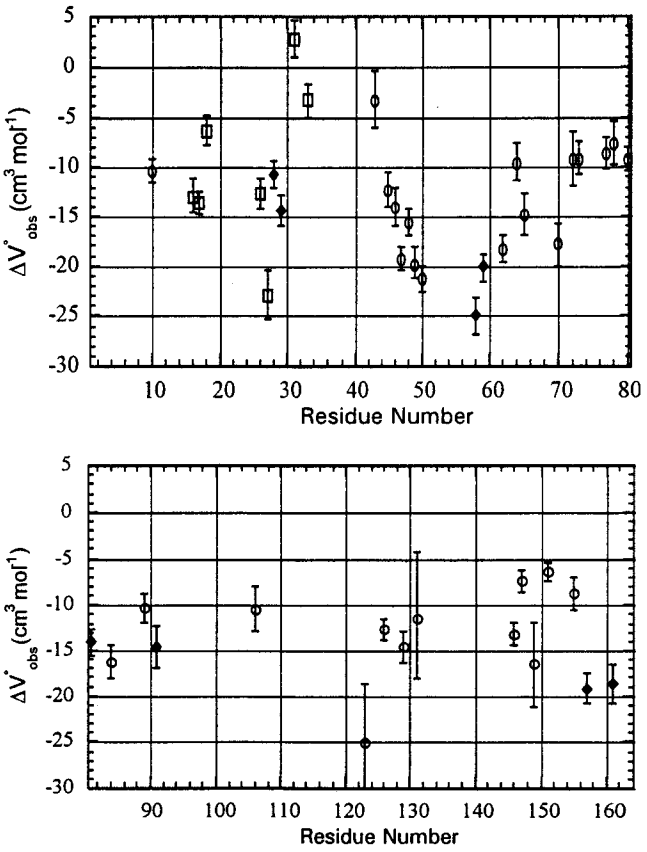

FIGURE 6: Activation volumes for hydrogen−deuterium exchange of WT* T4 lysozyme determined by the response of amide exchange kinetics to pressure from 0.1 to 200 MPa. Measured activation volumes were determined with eq 1 using kinetic data acquired at nine pressures. Error bars represent a 67% confidence interval of the fit. The □ symbol indicates antiparallel β-sheet secondary structure; the ○ symbol indicates α-helical secondary structure, and the ◆ symbol indicates other forms of secondary structure.

open or accessible and closed or inaccessible states. A simplified solution can be obtained by applying the steady state approximation on the open form; the apparent first-order rate constant, k_{obs}, is derived with eq 3 (*29*, *30*)

$$k_{obs} = \frac{k_1 k_{OH}[OH^-]}{k_{-1} + k_{OH}[OH^-]} \quad (3)$$

With the additional assumption that $k_{-1} \gg k_{OH}[OH^-]$, eq 3 simplifies to

$$k_{obs} = \frac{k_1}{k_{-1}} k_{OH}[OH^-] = K_{eq} k_{OH}[OH^-] \quad (4)$$

where K_{eq} is the equilibrium constant for the reversible opening−closing event (*8*).

In contrast to the local unfolding model, the penetration model for the hydrogen exchange requires that the exchange with solvent occurs from a structure that closely resembles the native structure. The transient exposure of amide hydrogen atoms to solvent is presumed to be mediated by small structural fluctuations of many atoms about their average position, thought to be less than 1 Å in amplitude. Intramolecular hydrogen bonds are envisioned to vary greatly in donor and acceptor distance and geometry; however, there is no large deviation (unfolding) of the secondary structure assumed. Hydrogen bonds are thought to break and form very rapidly as the donor and acceptor atom positions fluctuate. Occasionally, the donor and acceptor groups form transient hydrogen bonds with a water molecule and hydrogen exchange may occur (*6*, *10*, *31*, *32*). In this case, the observed exchange rate constant may be written as

$$k_{obs} = \beta k_{ex} \quad (5)$$

where β is the probability for a specific site to be exposed to solvent or catalyst and may be made to contain one or more concentrations.

We utilize eq 4 to analyze the pressure dependence of the amide hydrogen exchange rate constants. At pH* 7.5, the chemical exchange is dominated by the base-catalyzed mechanism and the rate is first-order in deuterium oxide ion concentration ($[OD^-]$). The pH* of the solution was maintained at 7.5 over the entire pressure range in this study (up to 200 MPa) with 50 mM TRIS buffer. No correction for small changes in pH was applied to kinetic experiments at high pressure because the pK_a of this buffer is practically pressure insensitive in both H_2O (*33*) and D_2O (*34*). At 200 MPa of applied pressure, the pH of the solution will increase by less than 0.035 unit as a result of the pressure-induced changes in the pK_a of TRIS. Although the pH* of the solution is essentially fixed over all pressures achieved in these experiments, the pOH is not because K_w is a function of pressure. Substituting $[OD^-] = K_W 10^{pH}$ into eq 4 yields

$$k_{obs} = K_{eq} k_{OH} K_w 10^{pH} \quad (6)$$

Taking partial derivatives with respect to pressure gives

$$\left[\frac{\partial \ln(k_{obs})}{\partial P}\right]_T = \left[\frac{\partial \ln(K_{eq})}{\partial P}\right]_T + \left[\frac{\partial \ln(k_{OH})}{\partial P}\right]_T + \left[\frac{\partial \ln(K_w 10^{pH})}{\partial P}\right]_T \quad (7)$$

Thus, the observed activation volume for amide hydrogen exchange may have contributions from three sources

$$\Delta V^{\ddagger}_{obs} = \Delta V_s + \Delta V^{\ddagger}_{k_{OH}} + \Delta V_{K_w} \quad (8)$$

$\Delta V^{\ddagger}_{k_{OH}}$ is the activation volume of the base-catalyzed chemical exchange process, ΔV_{K_w} is the volume change associated with the ionization of water, and ΔV_s is the volume change associated with accessibility of solvent to the site of hydrogen exchange. This reaction volume is a result of the change in the partial molar volume of the protein as the local structure sensed at the amide site progresses to the exchange-competent form.

Values for ΔV_{K_w} are reported to be between −20.9 and −22.1 cm^3 mol^{-1} (*35*−*37*). The value of $\Delta V^{\ddagger}_{k_{OH}}$ is available from two sources. Carter et al. (*27*) estimated the base-catalyzed chemical exchange contribution to $\Delta V^{\ddagger}_{obs}$ to be 6 ± 1 cm^3 mol^{-1} on the basis of total tritium−hydrogen exchange measurements made up to 250 MPa at pH 3 and 2 °C on poly(DL-lysine) and oxidized ribonuclease A. More recently, Mabry et al. (*38*) reported that $\Delta V^{\ddagger}_{k_{OH}}$ for *N*-methylacetamide is 10.9 cm^3 mol^{-1} on the basis of NMR magnetization transfer experiments at pH 7.5 and 66 °C.

Although these values are not the same, their similarity suggests that the volume change associated with the base-catalyzed chemical exchange step in the protein is similar to that for an unprotected amide in solution. To estimate the volume change associated with the solvent, we assume the value of 10.9 $cm^3\ mol^{-1}$ for $\Delta V^{\ddagger}_{k_{OH}}$ based on Mabry's measurements for *N*-methylacetamide (*38*) and a value of $-20.9\ cm^3\ mol^{-1}$ for ΔV_{K_w}. Substitution and rearrangement of eq 7 gives

$$\Delta V_s = \Delta V^{\ddagger}_{obs} - (10.9\ cm^3\ mol^{-1}) - (-20.9\ cm^3\ mol^{-1}) \quad (9)$$

These corrections result in the addition of 10.0 $cm^3\ mol^{-1}$ to $\Delta V^{\ddagger}_{obs}$ which yields ΔV_s values, which are also shown in Table 1.

Application of eq 8 assumes that the amide hydrogen exchange may be described by a mechanism that is first-order in hydroxide ion concentration. This assumption is at least approximately valid for measurements made at pH values near 7. The parameter ($\Delta \log k_{obs}/\Delta pH$) has been shown to differ from unity on the basic side of the exchange rate minimum for individual residues in bovine pancreatic trypsin inhibitor (*31*) and in hen egg white lysozyme (*39*). In addition, deviation from a first-order pH dependence for individual residues in BPTI is consistent with a side chain ionization event affecting the exchange event (*40*). Further, this approach ignores any contribution to the exchange rate from direct reaction with water, which may make a contribution in some cases. Even though the rate constant for the water exchange path is 7−8 orders of magnitude smaller than that for the hydroxide-catalyzed path (*40*), accessibility of the neutral water molecule to the exchange site may be far greater than that for the charged species. These complications preclude a mechanistically more detailed interpretation of the data at this time. Despite these approximations, the values of ΔV_S are instructive.

Figure 7 is a representation of the solvent accessibility volumes, ΔV_s, superimposed on a backbone tracing of the T4 lysozyme structure. The size of the sphere indicates the relative magnitude of ΔV_s. A blue sphere indicates a negative volume, and a red sphere indicates a positive volume. This presentation of the data demonstrates that there are no trivial correlations between ΔV_s and secondary structural type, which could be expected, for example, if a major unfolding event were mechanistically dominant. It is interesting to note that under much more extreme conditions Wagner reports amide exchange activation volumes more than 10 times larger than those found here for several sites in bovine pancreatic trypsin inhibitor. As pointed out earlier, these conditions are consistent with a high-activation enthalpy pathway often identified with major unfolding events. The uniformly smaller magnitudes of the activation volumes measured in this work compared with the 60 °C, pH 8 data of Wagner imply that the proton exchange pathways are substantially different and that large structural rearrangements are not required for the exchange events monitored in this work at 22 °C and pH* 7.5.

$P\Delta V_s$ may be interpreted as the energy associated with what rearrangements in protein structure are necessary for the amide proton to exchange with the solvent proton pool. From the perspective of eq 4, this energy is associated with

FIGURE 7: ΔV_s for T4 lysozyme obtained using eq 9. The sizes of the spheres represent magnitudes of ΔV_s, and the red color indicates a positive sign. The spheres are centered about the amide nitrogen atom for each exchange site.

K_{eq} or the step creating accessibility to the amide site. A positive value of ΔV_s corresponds to a slower rate or less accessibility, while a negative value corresponds to a faster rate or greater accessibility. In the context of the penetration model, where there may be several penetration steps required for exchange of a particular site, ΔV_s is a measure of the volume change for the rate-limiting penetration event. Although both positive and negative values of ΔV_s are observed, changes in sign do not generally occur abruptly as a function of residue number in the primary sequence.

The concentration of blue spheres in the lower left part of Figure 7 corresponds to the minimum in activation volumes observed in Figure 6. The region of the protein between helix B and helix C is hydrophobic and includes a loop region in which two activation volumes were measurable. Another strongly hydrophobic region is the helix bundle, in which the amide proton exchange rates are slow and the accessibility volumes are relatively small. In the helix B−helix C region, the accessibility volumes are larger which may reflect that there is greater flexibility in this region than in the helix bundle.

Helix B. An interesting feature of the data is represented in Figure 8 which shows that the measurable values of ΔV_s are nearly a linear function of the residue number for the residues in helix B (residues 39−50). Helix B is partly exposed to solvent on one side and interacts with the β-sheet on the opposite side (*17*). Activation volumes for residues 39−42 and Ser44 were not reported because the exchange rates were too fast to be observed using these methods. The

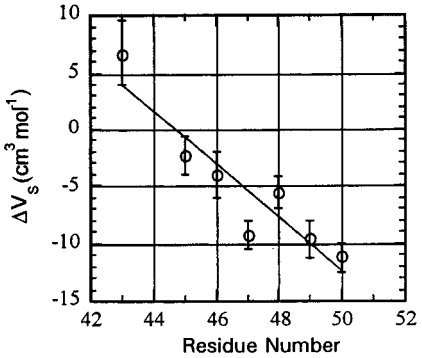

FIGURE 8: ΔV_s vs residue number for the sites measured in helix B of T4 lysozyme. Error bars represent a 67% confidence interval. The linear fit through the points has a slope of -2.3 cm^3 mol^{-1} residue^{-1}.

line through the data has a least-squares slope of -2.3 cm^3 mol^{-1} residue^{-1}.

The linear dependence of ΔV_s on increasing residue number suggests that there is an additive contribution to the activation volume that translates to an additive or linear contribution to the free energy of activation as one proceeds down helix B. There may be several origins of the effect. If an unfolding event, such as unwinding of the helix, is required for the solvent to access the next residue in the helix, the volume changes may be approximately additive down the helix. Noguchi and Jang (*41*) determined by dilatometry that the volume change for the helix−coil transition of polylysine is on the order of -1 cm^3 mol^{-1} residue^{-1}. This value is less than half the slope in Figure 8 which implies that other contributions are at least as significant.

Both the protection factors for amide proton exchange and the Debye−Waller or *B*-factors obtained from X-ray data suggest that the helix is conformationally more flexible near Leu39 and less flexible near Ile50. These trends are consistent with the dependence of ΔV_S on residue number. The region between helix B and helix C is hydrophobic. Conformational flexibility that permits hydrogen exchange may involve exposure of hydrophobic side chains with a concomitant contribution to ΔV_s from solvation changes. The change in partial molar volume per methylene unit is estimated from solute transfer experiments to be approximately -2.0 cm^3 mol^{-1} per methylene unit exposed (*42*). On the other hand, Prehoda and Markley (*43*) conclude that exposure of hydrophobic residues in a protein to solvent should result in a positive change in partial molar volume. Precise identification of contributions to ΔV_s is made more difficult by recognition that solvent electrostriction effects may be significant if not dominant (*35*). For example, if we assume that the solvated hydroxide ion catalyst must migrate from the bulk solvent, a region with a high dielectric constant, to an amide site in a region with a low dielectric constant, the result would be a negative volume change. The effective dielectric constant sensed at the exchange site may increase with increasing residue number as the hydrophobic region is approached, resulting in a dependence similar to that shown in Figure 8.

Helix C. There are nine residues in helix C for which activation volumes are determined. Five of these residues (Asp72, Ala73, Gly77, Ile78, and Arg80) are located near the hydrophobic core of the helix bundle. These five residues have small positive values of ΔV_s ranging from 0.8 to 1.5 cm^3 mol^{-1}. The slow amide hydrogen exchange rates of the surrounding residues suggest that this region of the protein is not rich in conformational fluctuations that permit solvent access for amide exchange. These small values of the activation volume are consistent with values estimated for breaking one hydrogen bond (*36*). One may speculate that the exchange of these sites may be mediated by small amplitude fluctuations that result in breaking a hydrogen bond that permits an exchange event. However, these small and similar values may also result from other more complex paths that involve considerable cancellation of contributions.

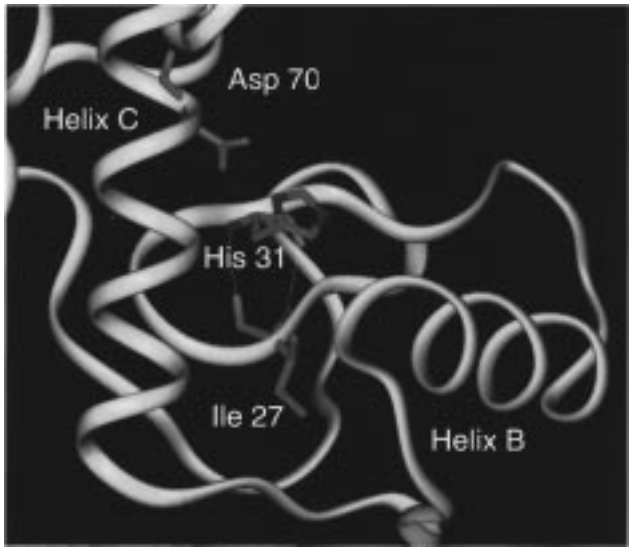

FIGURE 9: Expanded ribbon structure of T4 lysozyme. The heavy atoms for isoleucine 27, histidine 31, and aspartate 70 are shown. The histidine side chain forms a salt bridge with the side chain of aspartate 70. The backbone carbonyl and amide hydrogen of histidine 31 form two hydrogen bonds with the carbonyl and amide hydrogen of isoleucine 27 across the antiparallel β-sheet.

Histidine 31. The only amide exchange site that that has a positive measured activation volume $\Delta V^{\ddagger}_{obs}$ is histidine 31, which is unique in T4 lysozyme because the $N^{\delta 1}$−H of the side chain forms a salt bridge with the side chain of aspartate 70. This salt bridge is reported to contribute 3−5 kcal/mol to the free energy of the folded state (*16*). The pK_a of His31 has been estimated to be 9.1 in the folded state of the protein and 6.8 in the unfolded state created by 6 M urea at 10 °C and moderate salt. Mutation of aspartate 70 to aspargine results in a pK_a shift to 6.1 for the side chain of His31, which is a more normal value (*16*). Figure 9 shows the positions of Asp70 and His31 in the native fold of the protein. The crystal structure shows that Asp70 and His31 have small *B*-factors and are well ordered. The conditions of the current experiments place His31 in the acidic form. The pH is sufficiently far from the pK_a that ionization events should contribute little to the activation volume. Further, contributions from this ionization to $\Delta V^{\ddagger}_{obs}$ are expected to be small because, like TRIS buffer, the ionization does not increase the number of charges supported by the solvent. The salt bridge is accessible to solvent from one side and is placed in close proximity to the hydrophobic C-terminal domain. Histidine 31 is located in the antiparallel β-sheet region of the protein and forms a cyclic hydrogen bonding structure with Ile27 across the β-sheet. The ΔV_s values for these two closely related amide sites are markedly different. The ΔV_s for His31 is 12.8 cm^3 mol^{-1}, while ΔV_s for Ile27 is -12.9

$cm^3\ mol^{-1}$. The aspartic acid residue has a ΔV_s of -7.8 $cm^3\ mol^{-1}$. One might expect that, for residues such as His31 and Ile27, which form a cyclic hydrogen bonding interaction, the exchange of the two amide hydrogen atoms may be coupled to the same structural fluctuation. Exchange of one site, i.e., breaking one hydrogen bond, might facilitate breaking the other hydrogen bond and thus facilitate the exchange of the second amide hydrogen. If the same structural fluctuation were responsible for the exchange of the two structurally coupled residues, one could expect that the activation volumes would be similar. However, in this case, the values of ΔV_s are very different, which implies that other factors must dominate this observable value. One possible factor may be that steric constraints placed on the exchange events for these two residues differ considerably. For example, if the active exchange agent were required to approach from different sides of the β-sheet, substantially different activation volumes could result.

It is tempting to draw specific mechanistic conclusions based on relatively small differences between activation volumes; however, it is important to recognize that the pressure−volume changes make subtle contributions to the total energy of the exchange process. At the pH and temperature of these experiments, activation energies for amide hydrogen exchange are large, ranging from approximately 20 to 40 kcal/mol. However, the magnitude of $P\Delta V^{\ddagger}_{obs}$ is small at all pressures studied. For example, for a 10 mL/mol volume change, the energetic contribution at 200 MPa is about 0.5 kcal/mol. This value is far smaller than the other contributions to the barrier. This fact demonstrates that caution is required in making detailed mechanistic interpretations of the activation volumes in these different amide sites.

CONCLUSIONS

We have measured the pressure dependence of amide hydrogen exchange rates for 44 individual sites in T4 lysozyme. The analysis in terms of transition state theory has provided activation volumes for each of these positions in the folded protein. This extensive data set provides several important conclusions. (1) The observed activation volumes span the range from 2.75 to −25.1 mL/mol. When corrected for the pressure dependence of the ionic product for water, and for the reported activation volume for the amide exchange event in model compounds, the range is from −15.1 to 12.8 mL/mol. (2) There is no simple correlation between the activation volumes and the protection factors for amide proton exchange. (3) The activation volumes for residues near each other in the amino acid sequence may differ considerably. (4) There is no trivial correlation between the activation volume and the secondary structure unit in which a residue resides. (5) The activation volumes for residues that are apparently structurally coupled may be very different. (6) The small magnitudes of the activation volumes found are not consistent with major unfolding events appropriate for high-energy pathways appropriate under more extreme experimental conditions.

ACKNOWLEDGMENT

This work was submitted in partial fulfillment for the requirements of the Ph.D. degree for T.K.H. (University of Virginia, August 1997). We gratefully acknowledge the help of Frederick W. Dahlquist for making the T4 lysozyme plasmid available to us. We thank Gordon Rule for innumerable discussions about techniques, and we thank Rodney Biltonen, Clare Woodward, Rufus Lumry, and Wayne Bolen, with whom we have had helpful discussions about various aspects of this work. We thank Jason Jacobs for assistance in preparing the figures.

REFERENCES

1. Linderstrøm-lang, K. (1955) *Spec. Publ.—Chem. Soc. 2*, 1−24.
2. Hvidt, a., and Nielsen, S. O. (1966) *Adv. Protein Chem. 21*, 287.
3. Vas, M., and Boross, L. (1974) *Eur. J. Biochem. 43*, 237−244.
4. Lakowicz, J. R., and Weber, G. (1973) *Biochemistry 12*, 4171−4179.
5. Wüthrich, K., and Wagner, G. (1975) *FEBS Lett. 50*, 265−268.
6. Woodward, C., and Hilton, B. (1980) *Biophys. J. 32*, 561−575.
7. Hilton, B., Trudeau, K., and Woodward, C. (1981) *Biochemistry 20*, 4697−4703.
8. Englander, S. W., Downer, N. W., and Teitelbaum, H. (1972) *Annu. Rev. Biochem. 41*, 903−924.
9. Englander, S. W., and Kallenback, N. (1984) *Q. Rev. Biophys. 16*, 521−655.
10. Woodward, C., Simon, I., and Tüchsen, E., (1982) *Mol. Cell. Biol. 48*, 135−160.
11. Skinner, J. L., and Wolynes, P. G. (1978) *J. Chem. Phys. 69*, 2143−2150.
12. Karplus, M., and McCammon, J. A. (1981) *CRC Crit. Rev. Biochem. 9*, 293−235.
13. Munchmore, D. C., McIntosh, L. P., Russell, C. B., Anderson, D. E., and Dahlquist, F. W. (1989) *Methods Enzymol. 177*, 44−73.
14. Lu, J., and Dahlquist, F. W. (1992) *Biochemistry 31*, 4749−4756.
15. Fischer, M. W. F., Majumdar, A., Dahlquist, F. W., and Zuiderweg, E. R. P. (1995) *J. Magn. Reson., Ser. B 108*, 143−154.
16. Anderson, D. E., Becktel, W. J., and Dahlquist, F. W. (1990) *Biochemistry 29*, 2403−2408.
17. Mathews, B. W., and Remington, S. J. (1974) *Proc. Natl. Acad. Sci. U.S.A. 71*, 4178−4182.
18. Dahlquist, F. W. (1993) in *NMR of Proteins* (C. M. Clore and A. M. Gronenborn, Eds.) pp 256−304, CRC Press, Ann Arbor, MI.
19. Matsumura, M., and Matthews, B. W. (1989) *Science 243*, 792−794.
20. Bodenhausen, G., and Ruben, D. G. (1980) *Chem. Phys. Lett. 69*, 185−189.
21. Dahlquist, F. W. (1996) personal communication.
22. Vuister, G. W., and Bax, A. (1993) *J. Am. Chem. Soc. 115*, 7772−7777.
23. Jonhson, M. L., and Frasier, S. G. (1985) *Methods Enzymol. 117*, 301−341.
24. Wagner, G. (1982) *Commun. Mol. Cell. Biophys. 1*, 261−264.
25. Wagner, G. (1983) *Q. Rev. Biophys. 16*, 1−59.
26. Hilton, B. D., and Woodward, C. K. (1979) *Biochemistry 18*, 5834−5841.
27. Carter, J. V., Knox, D. G., and Rosenberg, A. (1978) *J. Biol. Chem. 253*, 1947−1953.
28. Englander, S. W. (1975) *Ann. N.Y. Acad. Sci. 244*, 10−27.
29. McDaniel, D. H., and Smoot, C. R. (1956) *J. Phys. Chem. 60*, 966−969.
30. Hvidt, A. (1964) *C. R. Trav. Lab. Carlsberg 34*, 299−317.
31. Woodward, C. K., and Hilton, B. D. (1979) *Annu. Rev. Biophys. Bioeng. 8*, 99−127.
32. Tüchsen, E., and Woodward, C. (1985) *J. Mol. Biol. 185*, 421−430.

33. Neuman, R. C., Jr., Kauzmann, W., and Zipp, A. (1973) *J. Phys. Chem. 77*, 2687−2691.
34. Hitchens, T. K., and Bryant, R. G. (1998) *J. Phys. Chem. 102*, 1002−1004.
35. Isaacs, N. S. (1981) *Liquid Phase High Pressure Chemistry*, John Wiley and Sons, New York.
36. Morild, E. (1981) *Adv. Protein Chem. 34*, 93−166.
37. VanEldik, R., Asano, T., and LeNobel, W. J. (1989) *Chem. Rev. 89*, 549−688.
38. Mabry, S. A., Lee, B., Zheng, T., and Jonas, J. (1996) *J. Am. Chem. Soc. 118*, 8887−8890.
39. Pedersen, T. G., Thomsen, N. K., Andersen, K. V., Madsen, J. C., and Poulsen, F. M. (1993*) J. Mol. Biol. 230*, 651−660.
40. Gregory, R. B., Crabo, L., Percy, A. J., and Rosenberg, A. (1983) *Biochemistry 22*, 910−917.
41. Noguchi, H., and Jang, J. T. (1971) *Biopolymers 10*, 2569−2579.
42. Visser, A. J. W. G., Li, T. M., Drickamer, H. G., and Webber, G. (1977) *Biochemistry 16*, 4883−4886.
43. Prehoda, K. E., and Markley, J. L. (1996) in *High Pressure Effects in Molecular Biophysics* and Enzymology (Markely, J. L., Northrop, D. B, and Royer, C. A., Eds.) pp 33−43, Oxford University Press, New York.

BI972950B